Origin of Optical Excitations in Fluorine-Doped Titania from 2 Response Function Theory: Relevance to Photocatalysis

4 AUTHORS, INCLUDING:

Sergio Tosoni
Università degli Studi di Milano-Bicocca
38 PUBLICATIONS **715** CITATIONS

SEE PROFILE

Daniel Fernandez Hevia
Universidad de Las Palmas de Gran Canaria
36 PUBLICATIONS **314** CITATIONS

SEE PROFILE

Oscar M González Díaz
Universidad de Las Palmas de Gran Canaria
130 PUBLICATIONS **1,216** CITATIONS

SEE PROFILE

Origin of Optical Excitations in Fluorine-Doped Titania from Response Function Theory: Relevance to Photocatalysis

Sergio Tosoni,[†,‡] Daniel Fernandez Hevia,[‡,§] Óscar González Díaz,[‡] and Francesc Illas*,[†]

[†]Departament de Química Física & Institut de Química Teòrica i Computacional (IQTCUB), Universitat de Barcelona, C/Martí i Franquès 1, E-08028 barcelona, Spain

[‡]Departamento de Química, Universidad de Las Palmas de Gran Canaria, Campus Universitario de Tafira, 35017 Las Palmas de Gran Canaria, Spain

[§]INAEL Electrical Systems S.A., C/Jarama 5, 45007 Toledo, Spain

Ⓢ Supporting Information

ABSTRACT: We investigate the effect of fluorine doping on the optical spectra of stoichiometric and reduced TiO_2 anatase, brookite, and rutile using density functional methods. The present approach is able to reproduce the main features of experiments and high-level quasiparticle calculations for undoped titania but at a much lower computational cost, thus allowing the study of doped titania, which requires large supercells. Whereas the simulated spectra of F-substituted brookite and rutile do not show any significant new feature, a relatively intense new band near the visible region is predicted for F-substituted anatase. This allows one to suggest assigning the spectral features near the visible region, observed on multiphase F-doped titania samples, to the presence of anatase. The physical origin of the new absorption band in F-doped anatase is unambiguously attributed to the presence of Ti^{3+} centers.
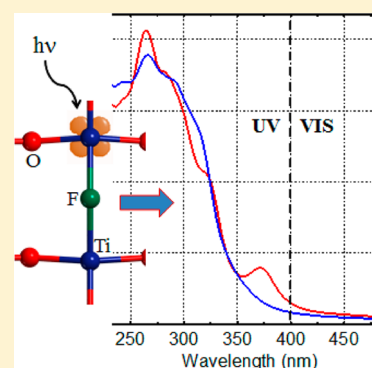
SECTION: Plasmonics, Optical Materials, and Hard Matter

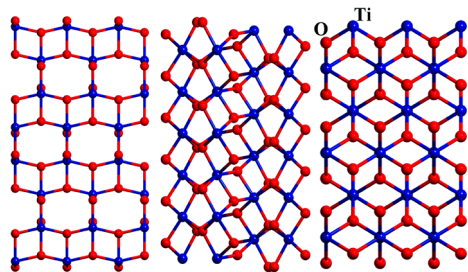The importance of titania (i.e., titanium dioxide, TiO_2) is due to its potential use in connection with either UV–visible light induced photocatalysis or solar cells.[1] Indeed, the photocatalytic properties of UV-irradiated titania toward water splitting and decomposition of organic molecules have been exhaustively described and reviewed.[2,3] The main steps of the mechanism behind these phenomena are known:[1,3] an incident photon of energy equal to or greater than the band gap of titania promotes an electron from the valence band to the conduction band. The promoted electron has a high reducing potential, whereas the corresponding photogenerated hole is strongly oxidant, thus giving rise to a variety of chemical reactions at the interface between titania and the external environment. Less is known, however, about the relationship between these phenomena and the microscopic structure of titania and, in particular, the different activity of its polymorphs and surfaces.[4] A problem of paramount importance, hindering the practical application of titania in photocatalytic devices, is its rather large band gap (close to 3 eV).[2] Such a large energy to promote electronic transitions limits the catalytic efficiency of TiO_2 when exposed to sunlight, because only a small percentage of the incident photons have sufficient energy to generate an electron-hole pair.[5] The most explored way to reduce the band gap of titania is doping with electron donors (for instance nitrogen in anatase)[6–11] aimed at introducing and populating gap states and thus reducing the energy required to promote electronic transitions.[1] In particular, there is evidence of photocatalytic activity of fluorine-doped TiO_2 under both UV[12] and visible light.[13] In addition, fluorine seems to act as a capping agent, stabilizing the highly reactive (001) anatase facets.[14,15] The complexity of the system and the difficulties to carry out controlled experiments of the doped materials hinder reaching a more detailed description of these systems. Theoretical studies based on quantum chemical simulations can contribute to understanding the relationship between these important properties and the chemical and electronic structure of titania, also providing valuable indications toward the synthesis of more efficient photocatalysts.
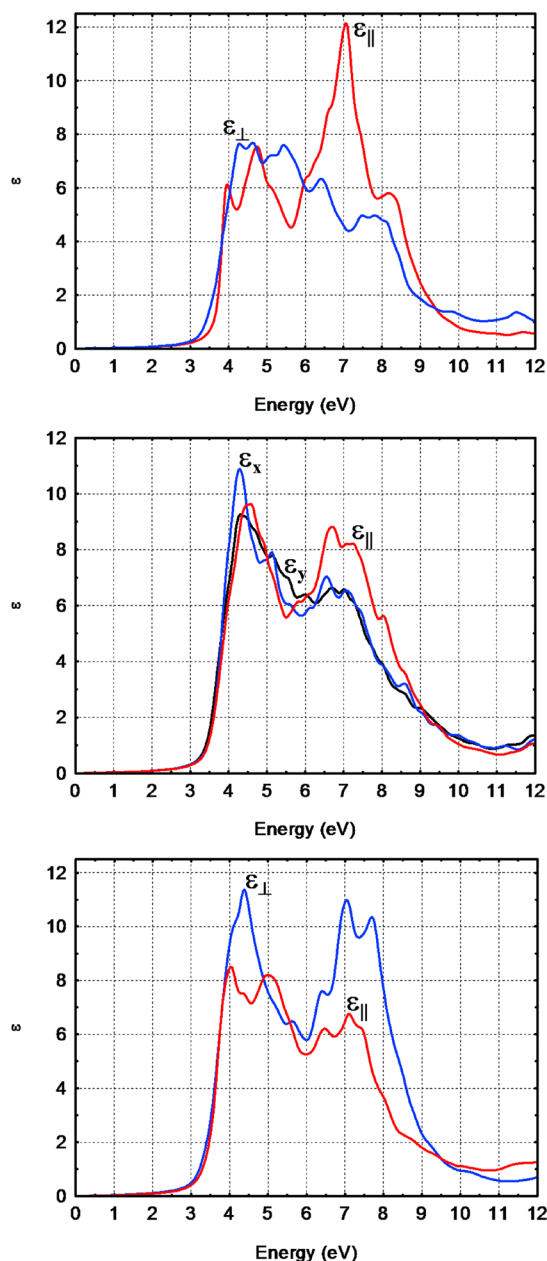
Under the perspective of potential industrial applications of doped titania, it is necessary to take into account the degree of complexity arising from synthesis under nonideal conditions, which leads to nanoparticles where microcrystalline domains of anatase, brookite, and rutile coexist in variable relative concentrations, depending on the synthesis conditions.[16–20] In this letter, we account for this complexity by studying periodic models of all three polymorphs separately. In particular, we adopt supercells large enough to keep the concentration of F close to 1% ($Ti_{48}O_{96}$ for anatase and rutile, $Ti_{54}O_{108}$ for brookite). The structures of the three polymorphs are displayed in Figure 1.

Figure 1. Anatase (left), brookite (middle), and rutile (right) oriented perpendicularly to the [010] direction.

In a previous work,[21] we discussed in detail the electronic structure of F-doped bulk polymorphs, considering O by F substitution in both stoichiometric and reduced structures, looking at density of states plots and of spin density maps. It was predicted that F−O substitution, as well as the reduction of titania (i.e., the removal of an oxygen atom) leads to the formation of localized Ti^{3+} centers in anatase, brookite, and rutile. In anatase and brookite, this turns into the appearance of populated states in the gap between the valence and the conduction band. In the case of rutile, the Ti^{3+} states lie very close to the valence band. It must be pointed out, however, that the adopted computational setup reasonably reproduces the band gap between O(2p) and Ti(3d) levels in the three polymorphs. However, this is at the expense of locating the Ti^{3+} states in reduced anatase too close to the valence band compared with the available experimental results.[22] In the present letter, we go one step further and present simulated UV−vis spectra obtained from the calculation of the dielectric function, whose main features are found not to depend on the particularities of the used computational method. (See the Supporting Information). This allows one to investigate the intensity of electronic transitions potentially relevant to photocatalysis and also to suggest assignment to features seen in some of the available experiments.

The electronic structure and optical response of titania have been described very recently by Landmann et al.,[23] who used high-quality time-dependent DFT calculations in the framework of the quasiparticle excitation G_0W_0 method combined with the Bethe−Salpeter Equation (BSE). These authors achieved a very good agreement between their BSE calculations and the experimental polarized resonance measurements on anatase[24] and rutile.[25] This approach is physically more complete than the one used in the present work because it accounts for excitonic contributions and local field effects, whereas in the present calculations one barely corrects for the self-interaction error of GGA by means of an empirical parameter. Nevertheless, the BSE-based method implies an extremely high computational cost, which hinders its applications to large supercells, such as the ones adopted for F-doped titania in the present work. We therefore use BSE results from Landmann et al.[23] as a benchmark to asses our data on undoped titania critically before proceeding to analyze data on doped models.

Because the imaginary part of the dielectric function contains the information about intensities and energies of the optical excitations, it is often referred to as optical response function. Figure 2 displays the calculated optical response function for undoped anatase, brookite, and rutile.

Because anatase and rutile are tetragonal, they show two-axial optical response functions with orthogonal ($\varepsilon_\perp$) and parallel

Figure 2. Frequency-dependent optical response function for anatase (top), brookite (middle), and rutile (bottom) as a function of the energy.

($\varepsilon_\parallel$) components with respect to the incident radiation. Brookite, on the contrary, is orthorhombic, and therefore $\varepsilon_\perp$ splits into two separated contributions, ε_x and ε_y. However, because of difficulties in synthetizing brookite single crystals, there are no experimental data available for direct comparison, and hence, the present calculations may also be helpful to provide to experimentalists this information. For anatase and rutile, a remarkable anisotropy is observed (Figure 2), and the absorption edge of $\varepsilon_\perp$ is red-shifted compared with that of $\varepsilon_\parallel$. The same is observed for brookite, even though in this case the effect is smaller. This observation is in agreement with polarized optical transmission measurements on anatase and rutile[26] and also with previous hybrid functional DFT calculations for anatase.[10]

We now attempt to extract further physically meaningful information by analyzing the different peaks of the optical

response function of anatase, brookite, and rutile. The most evident feature of the experimental optical response of anatase is a very sharp peak in ~4 eV in $\varepsilon_{\parallel}$.[24] In the simulated spectra reported in Figure 2 this feature is very well-reproduced with a peak at 3.9 eV, slightly red-shifted with respect to experiment. Likewise, the experimental $\varepsilon_{\perp}$ is characterized by a triplet centered between 4 and 6 eV, which is well-recognizable in Figure 2 at an energy range between 4.3 and 5.4 eV. Similarly to anatase, brookite shows a peak in $\varepsilon_{\parallel}$ centered around 4.5 eV although it is blue-shifted and broader than that predicted for anatase. It is remarkable that this spectral feature agrees with the one obtained by Landmann et al.[23] using the BSE. Continuing with brookite, $\varepsilon_{\perp}$ is split in two independent ε_{x} and ε_{y} contributions, both exhibiting a triplet shape spanning from 4.3 to 5.6 eV, which again agrees with the values reported by Landmann et al.[23] Finally, the measured optical response of rutile[25] displays a first sharp peak around 4.5 eV for $\varepsilon_{\perp}$, which is also present in the simulated spectra in Figure 2, where a strong peak is visible around 4.3 eV, although the calculated peak looks broader than the experimental one and its intensity is underestimated. For $\varepsilon_{\parallel}$, the experiment shows a doublet centered at ~5 eV, a feature that is reproduced by the BSE calculations of Landmann et al.[23] and also by the simpler present approach, although in our case the doublet is centered at lower energies, that is, 4.5 eV.

A comparison of the low energy features of the simulated spectra in Figure 2 to available experiments and high-quality calculations shows that the present computational scheme is able to describe adequately the edge of the optical absorption of titania at an affordable computational cost that allows consideration of complex (doped) systems. However, it is important to point out that whereas the quality of the agreement is good for the first peaks it becomes less accurate when higher energy features are considered. Nevertheless, the most interesting spectral features of doped titania are the energy of the transitions accountable for the UV−vis absorption edge. Therefore, we proceed with the analysis of the optical response spectra of F-doped stoichiometric and reduced titania. In the following, stoichiometric structures where F is substituting for lattice O atoms are referred to as F-anatase, F-brookite, and F-rutile, respectively. Reduced structures are obtained by removal of a lattice O atom and referred to as O-anatase, O-brookite, and O-rutile. O by F substitution in reduced titania leads to OF-anatase, OF-brookite, and OF-rutile.

To analyze the effect that F doping introduces in the spectra of stoichiometric or reduced TiO_2 samples, we take advantage of the previous experimental work of Yu et al.,[12] where the UV−vis absorption spectra of the titania-based Degussa P-25 catalyst are compared with those of F-doped nanocrystalline samples. Upon F doping, a remarkable red shift of the absorption band edge relative to that of titania-based Degussa P-25 catalyst was measured; this is a strong indication that F-doping induces a reduction of the band gap. In particular, a broad absorption peak is reported around 380 nm, at the boundary between the UV and the visible region. However, one must advert that other studies on F-doped anatase do not report this red shift in the absorption edge upon doping.[27,28] The origin of this discrepancy might lie in structural differences between the experimental samples as well as different chemical treatments. In particular, samples that, according to refs 27 and 28, are treated with HF do not show any shift in the absorption edge, despite the documented presence of reduced Ti^{3+} centers.

On the contrary, samples treated with NH_4F clearly show a shifted absorption edge.[12,27] However, Yu et al.[12] attributed the shift to the presence of fluorine and found no evidence of the presence of nitrogen in the nanoparticles. On the contrary, the XPS spectra reported by Li et al.[27] show that upon treatment with NH_4F nitrogen is also present as dopant in titania and relate the observed shift to N-doping. In the present letter we aim at contributing, at least partially, to the solution of this controversy, even though more work from both experiment and theory is necessary to account fully for these complex experimental results.

It is worth remarking that the experiments on fluorine-doped titania reported by Yu et al.[12] were performed on nanoparticles where two distinct crystalline phases (namely, anatase and brookite) and presumably many structural defects are present. Therefore, it is convenient to modify the approach used slightly to simulate the spectra of pure titania polymorphs reported in Figure 2. To this end, the simulated optical spectra of F-anatase, F-brookite, F-rutile O-anatase, O-brookite, O-rutile, OF-anatase, OF-brookite, and OF-rutile have been obtained from the optical response function averaged over the three spatial directions, merging together orthogonal and parallel contributions. The same approach has been recently applied to investigate the optical spectra of N-doped anatase.[10] Figure 3 reports simulated optical spectra, obtained from the averaged optical response function, for substitutional F-doped stoichiometric titania (F-anatase, F-brookite, and F-rutile) and includes the ones corresponding to the undoped phases for comparison. In the case of brookite, F-doping hardly affects the absorption edge, which is shifted by only a few nanometers. A modest red shift of 30 nm is predicted for rutile. However, a completely different situation appears from anatase, which displays a new band around 370 nm, hence near the visible range, and with a remarkable intensity. This feature is also visible in the experimental spectra reported in ref 12, where a first main peak emerges in the very same range of wavelength, even though our model does not fully account for the shape of the experimental spectra. This indicates that the accuracy of the present approach is quantitatively appreciable in predicting the transitions energies in the near UV region. Moreover, given the amorphous character of the samples, the experiments did not allow us to assign this new doping-related feature to either brookite or to anatase. The results in Figure 3 allow one to claim firmly that this observed feature near the visible is due the anatase phase in the experimental samples. However, neither the simulated spectra nor the experimental ones offer an explanation of the origin of this spectral feature.

To investigate further the physical origin of the new band induced by the presence of F in anatase, in Figure 4 we compare the simulated spectra of reduced titania (O-anatase, O-brookite, and O-rutile) and F-doped reduced titania (OF-anatase, OF-brookite, and OF-rutile). The case of O-brookite, O-rutile, OF-brookite, and OF-rutile does not bring any additional information. This is not the case for O-anatase, where OF-anatase give the same result as F-anatase in Figure 3, namely, a red shift of the absorption edge of the order of magnitude of 50 nm. The interesting point is, however, that this new optical absorption also appears in O-anatase, where there is no fluorine in the model. This is quite an unexpected result, providing strong evidence that the origin of this band is intrinsically due to the presence of Ti^{3+} centers, which are present in all three structures, as evidenced in the spin density plots reported in a previous study.[21]
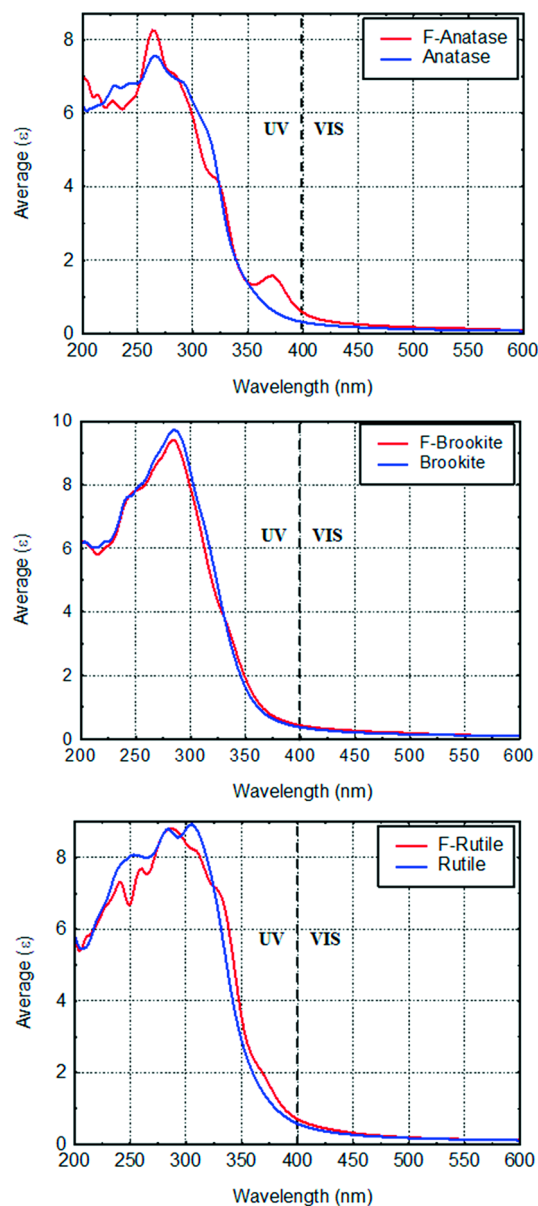
Figure 3. Frequency-dependent averaged optical response function for F-doped stoichiometric anatase (top), brookite (middle), and rutile (bottom).
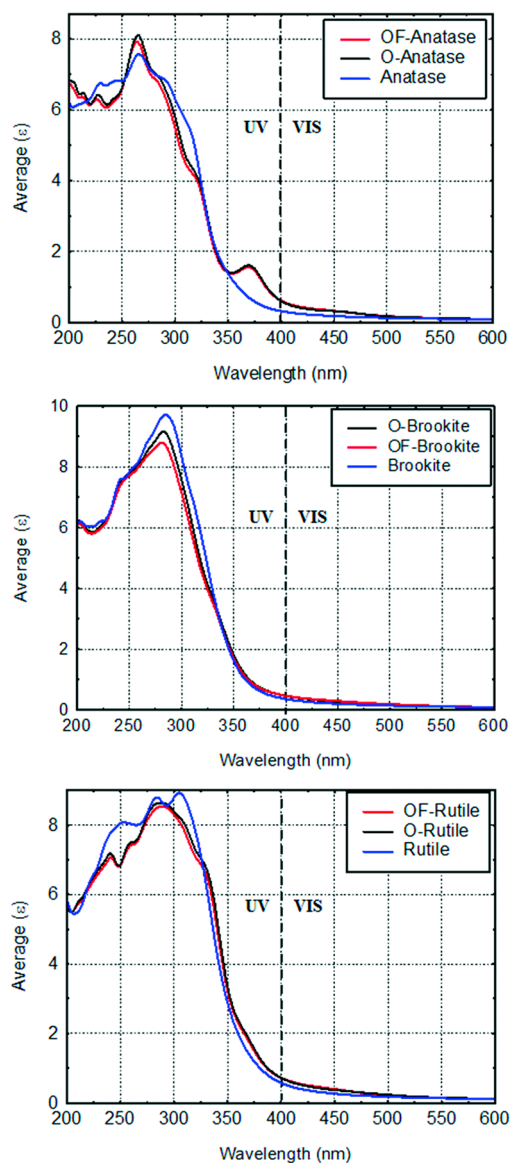
Figure 4. Frequency-dependent averaged optical response function for F-doped reduced anatase (top), brookite (middle), and rutile (bottom).

In conclusion, in the present letter we have shown that the dielectric function calculated at the PBE+U level, albeit not exact, accounts accurately for the optical properties of undoped titania. With this approach, we have calculated the spectra of stoichiometric and reduced F-doped titania, and we have found that the observed spectral features of mixed brookite-anatase samples are due only to the anatase component and the fact that the origin of this band lies intrinsically in the presence of Ti^{3+} centers.

■ COMPUTATIONAL METHODS

Density functional theory (DFT)-based calculations are carried out using the PBE functional.[29] The valence states of oxygen (2s, 2p), titanium (4s,3d), and fluorine (2s,2p) are expanded on a plane-wave basis set within an energy cutoff of 400 eV. The effect of the core states on the valence ones is introduced according to the projector augmented wave method.[30,31] The structures are relaxed within a gradient threshold of 0.005 eV/Å, and a grid of $2 \times 2 \times 2$ Monkhorst-Pack[32] special k-points is adopted for integration in the reciprocal space. To correct for the GGA intrinsic self-interaction error and thus penalize multiple occupancies,[33] we follow the DFT+U scheme proposed by Dudarev[34] and apply a Hubbard U term of 6 eV to both O(2s) and Ti (3d) states, as in our previous work.[21] It is worth to point out that this value for the U parameter has been chosen empirically to reproduce quantitatively the experimental band gap of pure rutile and anatase. A thorough discussion of the impact of U on the electronic structure of titania can be found in the recent work of Park et al.[35] Nevertheless, a systematic study, presented in the Supporting Information available for this manuscript, has been carried out, which shows that even if the precise location of the peaks of the undoped and F-doped titania depends on the value of U chosen to carry out the calculations the qualitative features and the existence of predicted peaks are not artifacts of a given choice of this parameter.

All calculations are performed with the code VASP 5.[36] The calculation of linear optical properties is done through the evaluation of the frequency-dependent dielectric function, as implemented in VASP.[37] This technique allows evaluating optical properties of complex materials qualitatively within the independent particle picture provided by the DFT based calculations.

■ ASSOCIATED CONTENT

S Supporting Information

■ AUTHOR INFORMATION

Notes

The authors declare no competing financial interest.

■ ACKNOWLEDGMENTS

■ REFERENCES

(1) Chen, X.; Mao, S. S. Titanium Dioxide Nanomaterials: Synthesis, Properties, Modifications, and Applications. *Chem. Rev.* **2007**, *107*, 2891–2895.

(2) Hashimoto, K.; Irie, H.; Fujishima, A. TiO_2 Photocatalysis: a Historical Overview and Future Prospects. *Jpn. J. Appl. Phys.* **2005**, *44*, 8269–8285.

(3) Fujishima, A.; Zhang, X.; Tryk, D. A. TiO_2 Photocatalysis and Related Surface Phenomena. *Surf. Sci. Rep.* **2008**, *63*, 515–582.

(4) Henderson, M. A. A Surface Science Perspective on TiO_2 Photocatalysis. *Surf. Sci. Rep.* **2011**, *66*, 185–297.

(5) Kudo, A.; Miseki, Y. Heterogeneous Photocatalyst Materials for Water Splitting. *Chem. Soc. Rev.* **2009**, *38*, 253–278.

(6) Di Valentin, C.; Pacchioni, G.; Selloni, A.; Livraghi, S.; Giamello, E. Characterization of Paramagnetic Species in N-doped TiO_2 Powders by EPR Spectroscopy and DFT Calculations. *J. Phys. Chem. B* **2005**, *109*, 11414–11419.

(7) Livraghi, S.; Paganini, M. C.; Giamello, E.; Selloni, A.; Di Valentin, C.; Pacchioni, G. Origin of Photoactivity of Nitrogen-Doped Titanium Dioxide Under Visible Light. *J. Am. Chem. Soc.* **2006**, *128*, 15666–15671.

(8) Di Valentin, C.; Finazzi, E.; Pacchioni, G.; Selloni, A.; Livraghi, S.; Paganini, M. C.; Giamello, E. N-Doped TiO_2: Theory and Experiment. *Chem. Phys.* **2007**, *339*, 44–56.

(9) Di Valentin, C.; Pacchioni, G.; Selloni, A. Reduced and N-Type Doped TiO_2: Nature of Ti^{3+} Species. *J. Phys. Chem. C* **2009**, *113*, 20543–20552.

(10) Harb, M.; Sautet, P.; Raybaud, P. Origin of The Enhanced Visible-Light Absorption in N-Doped Bulk Anatase TiO_2 from First-Principles Calculations. *J. Phys. Chem. C* **2011**, *115*, 19394–19404.

(11) Ceotto, M.; Lo Presti, L.; Cappelletti, G.; Meroni, D.; Spadavecchia, F.; Zecca, R.; Leoni, M.; Scardi, P.; Bianchi, C. L.; Ardizzone, S. About the Nitrogen Location in Nanocrystalline N-Doped TiO_2: Combined DFT and EXAFS Approach. *J. Phys. Chem. C* **2012**, *116*, 1764–1771.

(12) Yu, J. C.; Yu, J.; Ho, W.; Jiang, Z.; Zhang, L. Effects of F-Doping on the Photocatalytic Activity and Microstructures of Nanocrystalline TiO_2 Powders. *Chem. Mater.* **2002**, *14*, 3808–3816.

(13) Li, D.; Haneda, H.; Labhsetwar, N.; Hishita, S.; Ohashi, N. Visible-Light-Driven Photocatalysis on Fluorine-Doped TiO_2 Powders by the Creation of Surface Oxygen Vacancies. *Chem. Phys. Lett.* **2005**, *401*, 579–584.

(14) Yang, H. G.; Sun, C. H.; Qiao, S. Z.; Zou, J.; Liu, G.; Smith, S. C.; Cheng, H. M.; Lu, G. Q. Anatase TiO_2 Single Crystals with a Large Percentage of Reactive Facets. *Nature* **2008**, *453*, 638–641.

(15) Wu, X.; Chen, Z.; Lu, G. Q.; Wang, L. Nanosized Anatase TiO_2 Single Crystals with Tunable Exposed (001) Facets For Enhanced Energy Conversion Efficiency of Dye-Sensitized Solar Cells. *Adv. Funct. Mater.* **2011**, *21*, 4167.

(16) Yu, J. C.; Yu, J. G.; Ho, W. K.; Zhang, L. Z. Preparation of Highly Photocatalytic Active Nano-Sized. TiO_2 Particles via Ultrasonic Irradiation. *Chem. Commun.* **2001**, *19*, 1942–1943.

(17) Luo, H. M.; Takata, T.; Lee, Y. G.; Zhao, J. F.; Domen, K.; Yan, Y. S. Photocatalytic Activity Enhancing For Titanium Dioxide By Co-Doping With Bromine and Chlorine. *Chem. Mater.* **2004**, *16*, 846–849.

(18) Luo, H. M.; Wang, C.; Yan, Y. S. Synthesis of Mesostructured Titania with Controlled Crystalline Framework. *Chem. Mater.* **2003**, *15*, 3841–3846.

(19) Yu, J. G.; Xiong, J. F.; Cheng, B.; Liu, S. W. Fabrication and Characterization of Ag-TiO_2 Multiphase Nanocomposite Thin Films with Enhanced Photocatalytic Activity. *Appl. Catal., B* **2005**, *60*, 211–221.

(20) Yu, J. G.; Yu, J. C.; Leung, M. K. P.; Ho, W. K.; Cheng, B.; Zhao, X. J.; Zhao, J. C. Effects of Acidic and Basic Hydrolysis Catalysts on the Photocatalytic Activity and Microstructures of Bimodal Meso-porous Titania. *J. Catal.* **2003**, *217*, 69–78.

(21) Tosoni, S.; Lamiel-Garcia, O.; Fernandez Hevia, D.; Doña, J. M.; Illas, F. Electronic Structure of F-doped Bulk Rutile, Anatase and Brookite Polymorphs of TiO_2. *J. Phys. Chem. C* **2012**, *116*, 12738–12746.

(22) Henderson, M. A.; Epling, W. S.; Peden, C. H. F.; Perkins, C. L. Insights into Photoexcited Electron Scavenging Processes on TiO_2 Obtained from Studies of the Reaction of O_2 with OH Groups Adsorbed at Electronic Defects on TiO_2(110). *J. Phys. Chem. B* **2003**, *107*, 534–545.

(23) Landmann, M.; Rauls, E.; Schmidt, W. G. The Electronic Structure and Optical Response of Rutile, Anatase and Brookite TiO_2. *J. Phys.: Condens. Matter* **2012**, *24*, 195503.

(24) Hosaka, N.; Sekiya, T.; Satoko, C.; Kurita, S. Optical Properties of Single Crystal Anatase TiO_2. *J. Phys. Soc. Jpn.* **1997**, *66*, 877–880.

(25) Tiwald, T. E.; Schubert, M. Measurement of Rutile TiO_2 Dielectric Tensor from 0.148 to 33 μm Using Generalized Ellipsometry. *Proc. SPIE* **2000**, *4103*, 19–29.

(26) Tang, H.; Levy, F.; Berger, H.; Schmid, P. E. Urbach Tail of Anatase TiO_2. *Phys. Rev. B* **1995**, *52*, 7771.

(27) Li, D.; Ohashi, N.; Hishita, S.; Kolodiazhnyi, T.; Haneda, H. Origin of Visible Light-Driven Photocatalysis: A Comparative Study in N/F-Doped and N-F Codoped TiO_2 Powders by Means of Experimental Characterizations and Theoretical Calculations. *J. Solid State Chem.* **2005**, *178*, 3293–3302.

(28) Czoska, A. M.; Livraghi, S.; Chiesa, M.; Giamello, E.; Agnoli, S.; Granozzi, G.; Finazzi, E.; Di Valentin, C.; Pacchioni, G. The Nature of Defects in Fluorine-Doped TiO_2. *J. Phys. Chem. C* **2008**, *112*, 8951–8956.

(29) Perdew, J. P.; Burke, K.; Ernzerhof, M. Generalized Gradient Approximation Made Simple. *Phys. Rev. Lett.* **1996**, *77*, 3865–3868.

(30) Blöchl, P. Projector Augmented-Wave Method. *Phys. Rev. B* **1994**, *50*, 17953–17979.

(31) Kresse, G.; Joubert, J. From Ultrasoft Pseudopotentials to the Projector Augmented-Wave Method. *Phys. Rev. B* **1999**, *59*, 1758–1775.

E

dx.doi.org/10.1021/jz300870f | *J. Phys. Chem. Lett.* XXXX, XXX, XXX–XXX

428 (32) Monkhorst, H. J.; Pack, J. D. Special Points for Brillouin-Zone
429 Integrations. *Phys. Rev. B* **1976**, *13*, 5188−5192.
430 (33) Dagotto, E. Correlated Electrons in High-Temperature
431 Superconductors. *Rev. Mod. Phys.* **1994**, *66*, 763−840.
432 (34) Dudarev, S. L.; Botton, G. A.; Savrasov, S. Y.; Humphreys, C. J.;
433 Sutton, A. P. Electron-Energy-Loss Spectra and the Structural Stability
434 of Nickel Oxide: An LSDA+U Study. *Phys. Rev. B: Condens. Matter*
435 *Mater. Phys.* **1998**, *57*, 1505−1509.
436 (35) Park, S. G.; Magyari-Köpe, B.; Nishi, Y. Electronic Correlation
437 Effects in Reduced Rutile TiO_2 Within the LDA+U Method. *Phys. Rev.*
438 *B* **2010**, *82*, 115109.
439 (36) Kresse, G.; Furthmüller, J. Efficient Iterative Schemes for Ab
440 Initio Total-Energy Calculations Using a Plane-Wave Basis Set. *J.*
441 *Comput. Mater. Sci.* **1996**, *6*, 15−50.
442 (37) Gajdoš, M.; Hummer, K.; Kresse, G.; Furthmüller, J.; Bechstedt,
443 F. Linear Optical Properties in the Projector-Augmented Wave
444 Methodology. *Phys. Rev. B* **2006**, *73*, 045112.

F

dx.doi.org/10.1021/jz300870f | *J. Phys. Chem. Lett.* XXXX, XXX, XXX−XXX